PHYSICAL REVIEW C VOLUME 27, NUMBER 1 JANUARY 1983

Band structure and coupling modes in doubly-odd transitional $^{104\text{-}102}$Ag

J. Tréherne, J. Genevey, and S. André
Institut des Sciences Nucléaires, 38026 Grenoble Cedex, France

R. Béraud, A. Charvet, R. Duffait, A. Emsallem, and M. Meyer
Institut de Physique Nucléaire, Université Claude Bernard Lyon-1, 69622 Villeurbanne Cedex, France

C. Bourgeois, P. Kilcher, and J. Sauvage
Institut de Physique Nucléaire, Université Paris-Sud, 91406 Orsay Cedex, France

F. A. Beck and T. Byrski
Centre de Recherches Nucléaires, 67037 Strasbourg Cedex, France
(Received 28 May 1982)

Levels in ^{104}Ag and ^{102}Ag were studied using mainly the ^{94}Mo(^{12}C, pn) and the ^{89}Y(^{16}O, $3n$) reactions, respectively. A set of standard in-beam measurements involving relative excitation functions of γ rays, γ-γ-t coincidences, conversion electrons, angular distributions, and linear polarization of emitted γ rays have been performed. Excited states with spin values up to 17^- and 14^- are populated in ^{104}Ag and ^{102}Ag, respectively. The experimental data are discussed in the framework of the axial plus two quasiparticle model and some simple rules have been deduced to interpret the behavior of odd-odd transitional nuclei at high angular momentum.

NUCLEAR STRUCTURE ^{94}Mo(^{12}C,pn), $E=41-57$ MeV, ^{92}Mo(^{12}C,pn), $E=50$ MeV, ^{89}Y(^{16}O,$3n$), $E=60-80$ MeV, ^{92}Mo(^{14}N,$2p2n$), $E=72$ MeV; measured $I_\gamma[E(^{12}\text{C})]$, $I_\gamma[E(^{16}\text{O})]$, $I_\gamma(\theta)$, P_γ, γ-γ coin, $\gamma(t)$, E_{CE}, I_{CE}. ^{104}Ag and ^{102}Ag deduced levels, J, π, ICC, γ multipolarity, $t_{1/2}$. Enriched ^{92,94}Mo targets, Ge(Li) detectors, intrinsic Ge Compton polarimeter, electron orange spectrometer. Calculated levels from axial rotor plus two quasiparticle model.

I. INTRODUCTION

In recent years, a new interest has been devoted to odd-odd transitional nuclei. The investigation of the high-spin structure of such nuclei, which are especially sensitive to the Coriolis force according to the rotor plus quasiparticles model, presently looks rather attractive. The properties of the odd-mass transitional nuclei have already been discussed extensively. Let us recall that the coupling mode is mainly related to the value of the deformation, the subshell angular momentum j, and the component Ω of the angular momentum j on the symmetry axis. For small deformation, high-j shell, and low-Ω values, the odd particle prefers the decoupling scheme and its angular momentum j aligns along the rotation axis. On the other hand, high-Ω values (such as $\Omega=j$) give rise to strong coupling. Then the angular momentum j of the particle points along the symmetry axis. The extension of that picture to odd-odd nuclei is tempting. When both odd neutron and proton have similar coupling properties, the situation can be described in terms of a "peaceful scheme." The case of both strongly coupled particles is well known while that of decoupled particles is less trivial. However, in the frame of the axial rotor or triaxial rotor plus quasiparticles models, the odd-odd structure in the peaceful scheme can be represented by the two quasiparticles acting as a "super particle" according to Faessler.[1] A peaceful situation involving two decoupled particles ($\pi h_{11/2}{}^{-1}\otimes\nu i_{13/2}{}^{-1}$) has been already observed in the $^{190-194}$Au nuclei.[2] The problem remains open for the "conflicting case" where one particle is coupled whereas the other is decoupled. In the last few years, this case has been explored for $^{196-200}$Tl (Ref. 3) (decoupled neutron $\nu i_{13/2}$ and strongly coupled proton $\pi h_{9/2}$) and $^{110-108}$In (Refs. 4 and 5) (decoupled neutron $\nu h_{11/2}$

and strongly coupled proton $\pi g_{9/2}$). The main result of these experimental studies consists of a negative parity band based on a 7^- or an 8^- state arising from the conflicting coupling of the two quasiparticles to the core. The bandhead spin can be approximately obtained by using the relation $J=(j_n{}^2+j_p{}^2)^{1/2}$. In both regions, a $\Delta I=1$ band is built on states connected by strong $M1$ transitions. The rotor plus quasiparticles model can be applied to odd-odd Tl or In nuclei as well as for the neighboring odd-A nuclei. However, only one band has been firmly assigned up to now *in these nuclei* and several problems remain. In particular the origin of the energy level staggering must be cleared up: It could be due either to J dependence of the V_{pn} interaction or to Coriolis force. The configurations involved in the odd-odd Ag nuclei can be deduced from the structure of the adjacent odd-A nuclei. Odd-A Ag exhibit a $\Delta I=1$ strongly coupled (but perturbed) band based on a $\frac{9}{2}^+$ or $\frac{7}{2}^+$ state from $\pi g_{9/2}$.[6-8] On the other hand, odd-A Pd (Refs. 9 and 10) and Cd (Refs. 11–14) display a $\Delta I=2$ decoupled band based on an $\frac{11}{2}^-$ state from $\nu h_{11/2}$ and two others built on a $\frac{7}{2}^+$ state from $\nu g_{7/2}$ $(\Omega_\nu=\frac{1}{2},\frac{3}{2})$ and on a $\frac{5}{2}^+$ state from $\nu d_{5/2}$ $(\Omega_\nu=\frac{3}{2},\frac{5}{2})$ which are quasidecoupled and perturbed, respectively. However, the situation is slightly different for very neutron deficient nuclei. In ^{101}Pd, for example, the Fermi level lies near the $\Omega_\nu=\frac{1}{2}$ orbital of $\nu d\frac{5}{2}$ and the $\frac{5}{2}^+$ band becomes decoupled like the two others. All these configurations are expected in the odd-odd Ag nuclei, which is confirmed in a recent investigation of ^{106}Ag.[5] In this nucleus, besides a $\Delta I=1$ negative-parity coupled band based on an 8^- state interpreted in terms of the $(\nu h_{11/2}\otimes\pi g_{9/2})$ configuration, two $(\Delta I=1+\Delta I=2)$ positive parity perturbed bands are built on 8^+, 7^+ states corresponding to $(\nu g_{7/2}\otimes\pi g_{9/2}),(\nu d_{5/2}\otimes\pi g_{9/2})$ configurations and a decoupled $\Delta I=2$ band arises from the $(\nu h_{11/2}\otimes\pi p_{1/2})$ configuration. It is important to know the behavior of such bands in the more neutron deficient odd-odd nuclei in order to get valuable information on the coupling schemes and on the V_{pn} interaction. For that purpose, the study of the high-spin structure of ^{102,104}Ag has been undertaken in the present work. In Secs. II and III are given the experimental procedure and data. In Sec. IV, the results are discussed in the framework of the "axial rotor plus two quasiparticle" model. From the striking analogy between odd and doubly-odd Ag band structure, we can state simple rules guiding the "conflicting case."

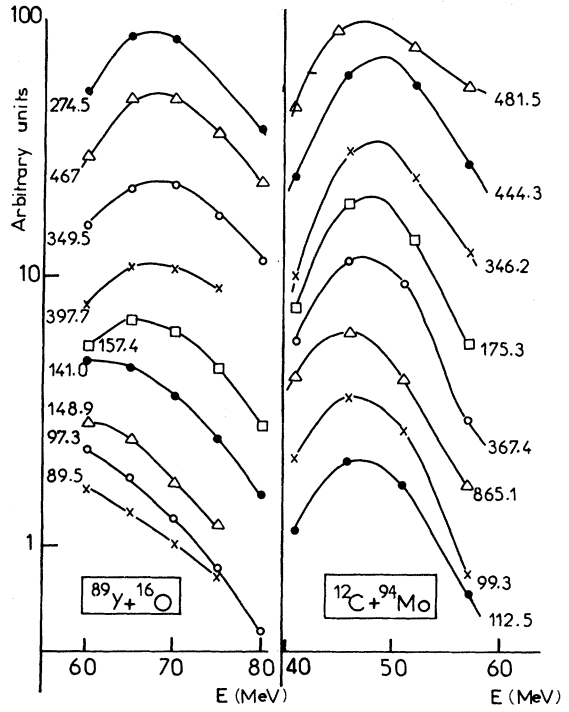

FIG. 1. Relative yield of γ intensity as a function of bombardment energy for some low-energy γ rays and transitions occurring in the negative parity cascade of ^{102}Ag and ^{104}Ag.

II. EXPERIMENTAL PROCEDURE AND RESULTS

Most of the experimental results have been obtained at the Grenoble isochronous cyclotron and at the Orsay tandem accelerator. Some γ-ray linear polarization experiments have also been performed at the Strasbourg tandem accelerator.

The levels of ^{104}Ag were excited through the ^{94}Mo(^{12}C,pn) reaction at 50 MeV. In order to clear up some discrepancies, various reactions such as ^{89}Y(^{16}O,3n) at 60 MeV, ^{92}Mo(^{14}N,2p2n) at 72 MeV, and ^{92}Mo(^{12}C,pn) at 50 MeV have been used to excite high spin levels in ^{102}Ag. The ^{92}Mo and ^{94}Mo targets (both enriched to 98%) were 4 mg/cm^2 thick. For electron spectroscopy, self-supporting foils of 1 mg/cm^2 were used.

The experimental procedures are those commonly used in usual in-beam spectroscopy. The measurements included γ-ray intensities as a function of beam energy, γ-γ-t coincidences, γ-ray angular distributions, γ-ray linear polarization, conversion electron intensity, and timing measurements. Let us mention the use of a special Compton polarimeter composed of five intrinsic Ge detectors and described in Ref. 16. Conversion electron experiments have been carried out using the in-beam Grenoble orange spectrometer previously described.[17]

TABLE I. Relative γ-ray intensities of ^{102}Ag from the reactions $^{16}O + ^{89}Y$ at 60 MeV, $^{14}N + ^{92}Mo$ at 72 MeV, and $^{12}C + ^{92}Mo$ at 50 MeV. All intensities have been corrected for detector efficiencies, target absorption in case of low-energy γ lines, and the angular distribution effect. The following γ lines were not placed in our level scheme: 236, 261, 482, and 487 keV. The asterisk indicates mixed transitions.

Transition energy (keV)	Relative intensity $^{16}O + ^{89}Y$	$^{14}N + ^{92}Mo$	$^{12}C + ^{92}Mo$	Transition energy (keV)	Relative intensity $^{16}O + ^{89}Y$	$^{12}C + ^{92}Mo$	Transition energy (keV)	Relative intensity $^{16}O + ^{89}Y$	$^{12}C + ^{92}Mo$
40.0	100	70		336.1		30	745.7	5.8	6.3
45.9	23	21		349.5	22	12	748.0	11	4
58.9	weak	0.6		397.7	<31	17	816.5		10
89.5	15	17	26*	415.1		10	819.4	10	16
97.3	15	18	56*	463.4	5.3	10	839.1	~ 80	60
129.7	3.7	0.8		466.4	34	17	860.9	~ 20	5.5
141.0	100	100	100	467.6			875.9	41	25
148.9	21	24	34	482	weak	4	951.0	29	15
157.4	26	30	15.4	487	weak	<10	1084.0		weak
174.5	6.7	6.4	12.7	539.8	14*	28	1147	weak	3.1
186.8	4.9	10	15	555.1		1.3	1183.4		10
195.6	3.1	11	8	637.0	8	5	1367.8	~ 12	16
236	weak								
261	weak								
274.5	20*	26*	17*	664.6	27	15			
279.1	4.3	4.3	12	705	≤ 7	3			

Prompt and delayed γ-ray spectra were measured at different bombardment energies ranging from 60 to 80 MeV for the $^{89}Y(^{16}O,3n)^{102}Ag$ reaction and from 41 to 57 MeV for the $^{94}Mo(^{12}C,pn)^{104}Ag$ reaction. Some excitation function curves are shown in Fig. 1. It should be noted that the maximum yield of transitions between low-spin states is shifted towards low bombardment energies especially in the case of ^{102}Ag. γ rays have been assigned to ^{102}Ag and ^{104}Ag on the grounds of excitation function results.

In Table I are listed the energies and intensities of ^{102}Ag γ rays observed via both $^{92}Mo + ^{12}C$ 50 MeV and $^{89}Y + ^{16}O$ 60 MeV reactions. In addition the results of the $^{92}Mo + ^{14}N$ 72 MeV reaction are given for the low-energy γ rays (up to 300 keV) detected with an x-ray Ge detector. In Table II are given the γ lines ascribed to ^{104}Ag in the $^{94}Mo + ^{12}C$ reaction at 50 MeV, with their intensities. In order to establish the level schemes, biparametric $2K$-$2K$ channel coincidence measurements have been carried out with a time resolution of about 15 ns. In Figs. 2–4 are shown typical examples of gated spectra. More convincing data can be obtained by summing some crucial gates, and the resulting spectra are also displayed. Spins and parities have been assigned on the basis of angular distribution, linear polarization, and conversion electron measurements. Angular distributions have been performed at five different angles (0°, 22°, 45°, 67°, and 90°) with respect to the beam direction. The centering corrections were performed by counting the radioactivity at the end of the measurements. The γ-ray linear polarizations were obtained using the polarimeter already mentioned. The experimental value of the polarization p was deduced for intense γ rays from the coincidences scattered plus horizontal (N_{hor}), and scattered plus vertical (N_{ver}) through the relation

$$p = \frac{1}{Q(E_\gamma)} \frac{N_{ver} - N_{hor}}{N_{ver} + N_{hor}},$$

where $Q(E_\gamma)$ is the polarization sensitivity of the polarimeter given in Ref. 16 with a detailed description of the setup and calibration procedure. Results of angular distributions and linear polarizations are given in Tables III and IV. Simultaneous fits to the angular distribution coefficients and to the linear polarization data, versus the nuclear spin alignment and the mixing ratio values, allowed unique spin and parity assignments for the majority of the levels. The mixing parameter δ is defined for emission radiation and is in the phase convention of Biedenharn and Rose.[18] Extreme values of δ were deduced from fits taking χ^2 values corresponding to 0.1% confidence level. The mixing ratios deduced from α_K or α_L values are generally in good agreement; they are reported in Tables V and VI for ^{102}Ag and ^{104}Ag,

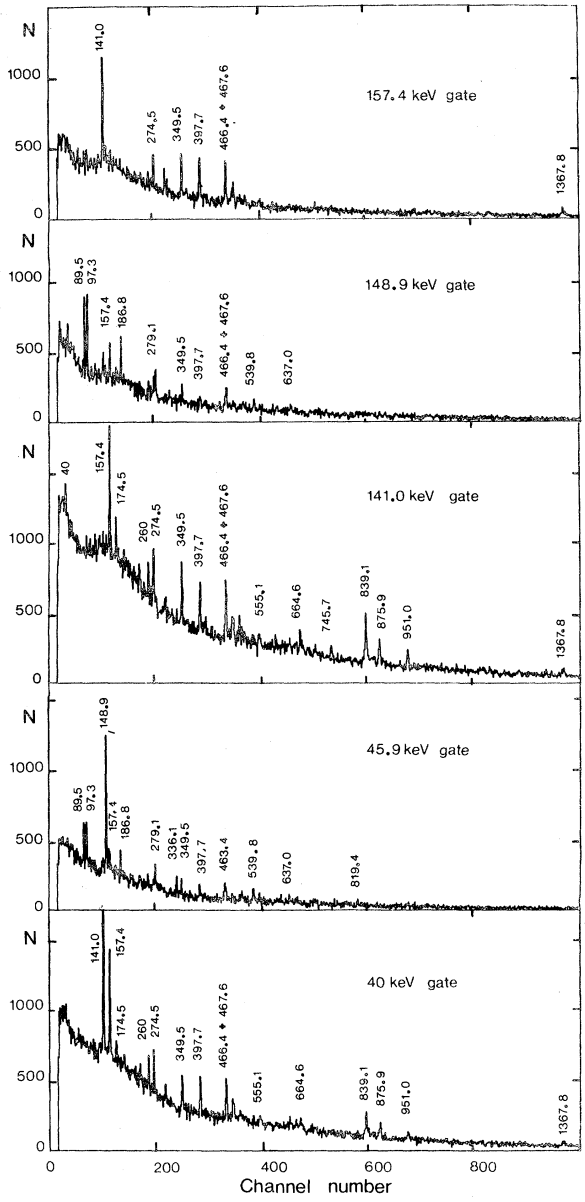

FIG. 2. Coincident γ-ray spectra measured in ^{102}Ag and gated on the X detector in the case of the reaction ^{89}Y + ^{16}O at 60 MeV.

respectively. The 40 and 141 keV transitions are both delayed as indicated by their intensity ratio in the "out of beam" spectra. The lifetime of the 181 keV level was measured from a beam-γ 141 keV time correlation spectrum and found to be $T_{1/2}=3.5\pm0.5$ ns (see Fig. 5).

III. LEVEL SCHEMES

A. ^{104}Ag

The ground state spin of ^{104}Ag ($I^{\pi}=5^{+}$) is well known from atomic beam measurements and decay studies. The main feature of the level scheme shown in Fig. 6 is the existence of a well-developed $\Delta I=1$ sequence of levels based on an 8^{-} state. In most cases, $\Delta I=2$ crossover transitions are observed more strongly than in some other odd-odd nuclei such as ^{108}In.[5] This band mainly deexcites through the 865.1 keV transition to the 7^{+} state, and partly through the (7^{-}) and (6^{-}) states. These two states and the 8^{-} one show a well-marked bunching as in ^{106}Ag.[15] The sequence of γ rays—175.3, 346.2, 332.7, and 444.3 keV—has been previously observed in the ^{103}Rh(α,3$n\gamma$)^{104}Ag study.[19] But this was assumed to be built on a 6^{+} or 7^{+} state due to the misplacing of the 865.1 keV transition and the lack of coincidence measurements set on 50.3 and 66.8 keV gates. In our experiment, with the ^{12}C projectiles, the $\Delta I=1$ sequence is more developed by a few units of angular momentum. Between this structure and the ground state "band" a number of low spin levels take place. At the right of the figure a positive parity band with spins 7^{+}, 9^{+}, 11^{+} is weakly populated, as in ^{106}Ag.

B. ^{102}Ag

The ^{102}Ag level scheme exhibits a structure similar to that observed in ^{104}Ag. However, the $13^{+}\rightarrow11^{+}\rightarrow9^{+}\rightarrow7^{+}$ sequence of levels appears as the strongest cascade whereas the negative parity band is shifted to higher energy. One has to point out that the 1367.8 keV transition cannot deexcite the intensity of the whole negative band. From coincidence measurements, about 20% of the 157.4 keV transition intensity feed the low-lying levels of another positive parity system (shown on the right side of Fig. 7) not observed in ^{104}Ag. This system, consisting of $\Delta I=1$ low energy transitions, already deexciting a positive parity perturbed band based on the 382.0 7^{+} state, is also fed by almost 30% of the 397.7 keV γ ray through the 860.9 and 463.4 keV transitions.

IV. DISCUSSION

In this section we shall discuss, from a systematic point of view, the structure of the three silver isotopes, $^{102}_{47}Ag_{55}$, $^{104}_{47}Ag_{57}$, and $^{106}_{47}Ag_{59}$, in the frame of the slightly deformed axial rotor plus two quasiparticles model.[5,15] This model has already been applied to the odd-odd ^{106}Ag nucleus by Popli *et al.*[15] using Nilsson states with the usual parameters δ,κ,μ; the Fermi surfaces λ_n,λ_p; and the pairing gaps Δn, Δp taking into account a variable moment of inertia of the core, a simple residual V_{pn} interaction, and expanding their deformed wave functions $|IMK\Omega_n\Omega_p\rangle$ on the quasispherical basis

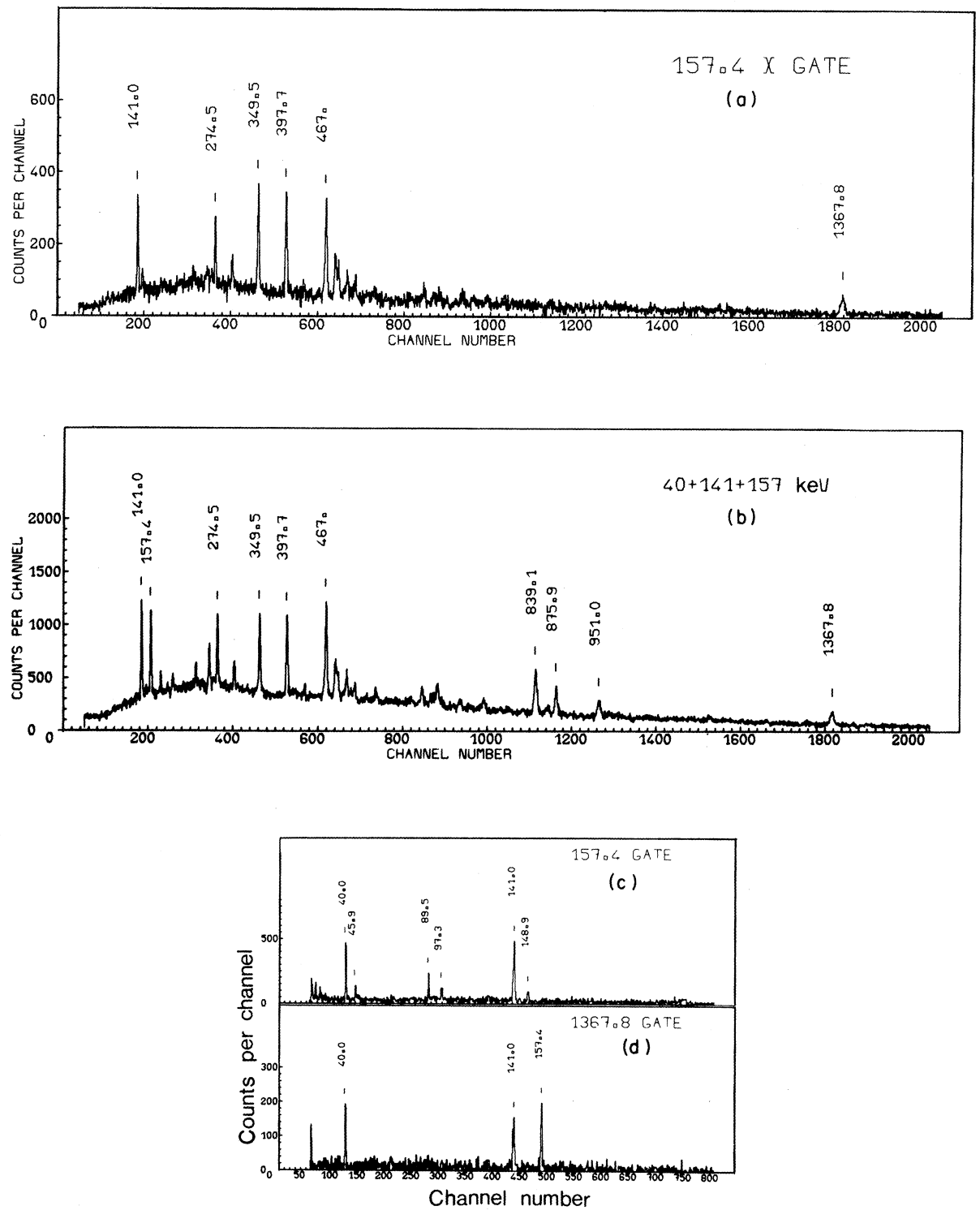

FIG. 3. Coincident γ-ray spectra from the reaction $^{92}Mo + ^{14}N$ at 72 MeV, measured in ^{102}Ag and gated on the detector by lines at (a) 157.4 keV and (b) the (40 + 141 + 157) keV group. (c) and (d) are low-energy spectra gated by 157.4 keV and 1367.8 keV γ lines.

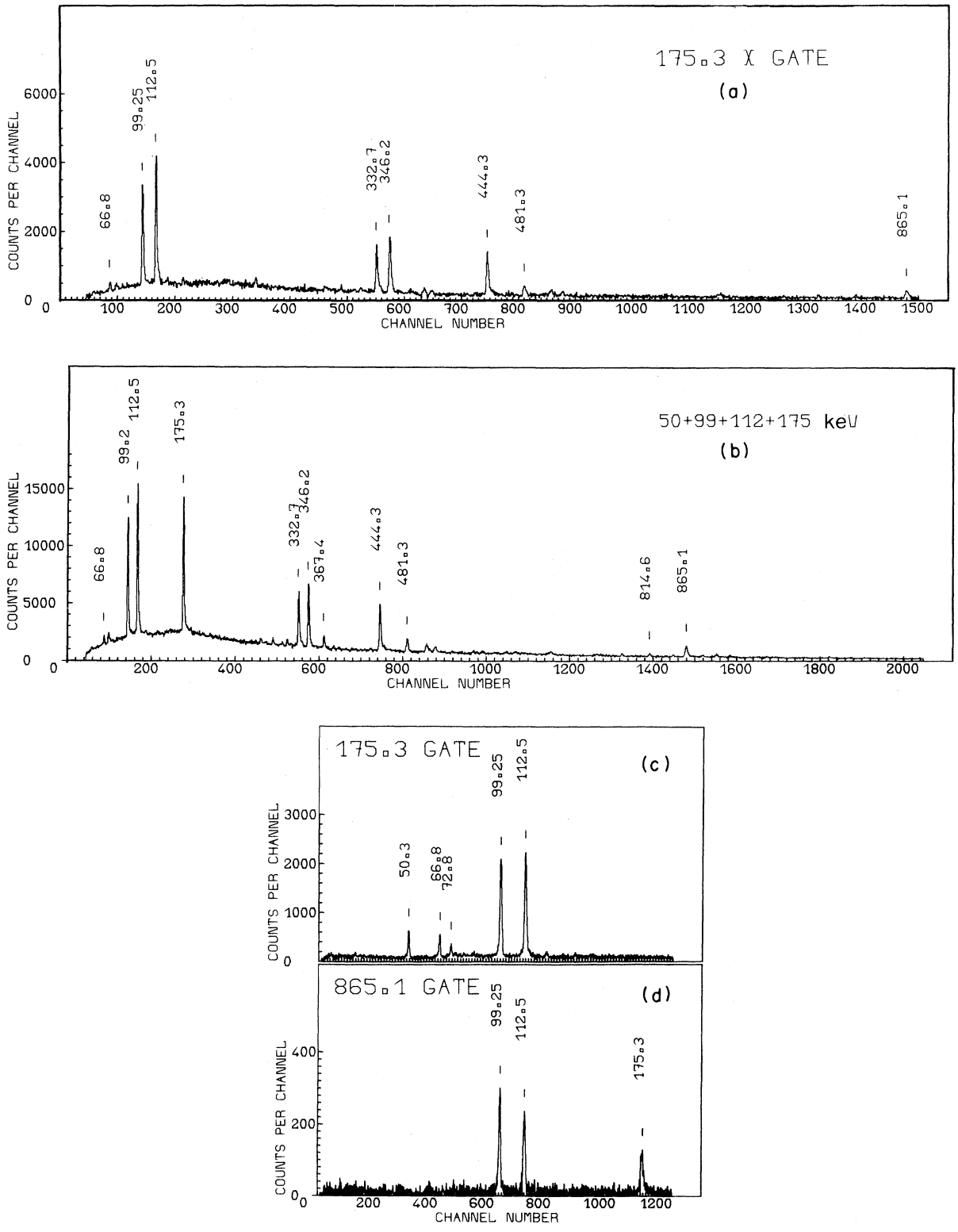

FIG. 4. Coincident γ-ray spectra measured in ^{104}Ag and gated on the detector by lines at (a) 175.3 keV and (b) the 50 + 99 + 112 + 175 keV group. (c) and (d) are low-energy parts of spectra gated by 175.3 and 865.1 keV γ lines. These spectra were observed in the reaction ^{94}Mo + ^{12}C at 50 MeV.

TABLE II. Energy and relative intensity of γ rays assigned to ^{104}Ag observed in the ^{94}Mo + ^{12}C reaction at 50 MeV. The lines marked with an asterisk are composite ones: The energies (of the order of 0.2 keV accuracy as for all the transitions) inside the unresolved doublets are very similar, as can be seen from the decomposition of the γ-rays spectra and coincidence gates. The lines marked (c) have been detected by coincidence measurements. The γ lines 75.0 and 296.5 keV are not placed in our level scheme.

Transition energy	Relative intensity	Transition energy (keV)	Relative intensity	Transition energy (keV)	Relative intensity
50.3	6(1)	316.7	8(2)	741.5 (c)	3(1)
66.8*	5(1)	321.6	4(1)	748.0 (c)	3(1)
66.8*	2(1)			777.0 (c)	10(2)
72.8	5(1)	332.7	33(4)	814.6	8(2)
75.0	3(1)	346.2	40(5)	847.2	9(2)
83.7 (c)	2(1)	367.4*	3(1)	848.0	~1
99.3	65(5)	367.4*	14.4(4)	865.1	30(5)
112.5	100	444.3*	40(4)	888.0 (c)	7(2)
		444.3*		906.8	20(3)
114.5	5(1)	481.3	19(2)	926.0 (c)	5(2)
123.8	5(1)	508.5	12(3)	990.0 (c)	5(2)
139.0	5(1)	520.7 (c)	10(3)	1028.0	4(2)
175.3	50(5)	570.1	3(1)	1062.0	12(2)
211.8	5(1)	575.9 (c)	~1		
219.0	1.0(0.5)	584.8	5(1)		
280.4 (c)	4(1)	675.0 (c)	3(1)		
296.5	4(1)	679.0 (c)	8(2)		

$|IMKJj_nj_p\rangle$. Three $\Delta I=1$ bands have been clearly identified by this model in ^{106}Ag as the $(vh_{11/2}\otimes\pi g_{9/2})$ system based on a 10^- state, $(vg_{7/2}\otimes\pi g_{9/2})$ on an 8^+ state, $(vd_{5/2}\otimes\pi g_{9/2})$ on a 7^+ state, and a $\Delta I=2$ decoupled one based on a 5^+ state as $(vh_{11/2}\otimes\pi p_{1/2})$. We also applied this axial rotor model plus two quasiparticles, but only in the usual standard basis $|IMK\Omega_n\Omega_p\rangle$ neglecting the residual V_{pn} interaction. The advantage of our calculations, already described in detail in Ref. 5, lies in the choice of the deformed single quasiparticle states: Our states, extracted at the minimum energy from the deformed Hartree-Fock calculation performed on a ^{106}Cd core,[20,21] are free of parameters. Such a calculation (^{106}Cd$+qp\pi+qpv$) is able to bring information from ^{104}Ag to ^{108}In because no projection has been performed on the number N of particles. For silver isotopes we obtained reasonable agreement, as will be discussed shortly, with an inertia parameter value $\hbar^2/2\mathcal{I}$ of 0.05 MeV. The silver nuclei seem a little more deformed than the indium ones but always with a prolate shape.

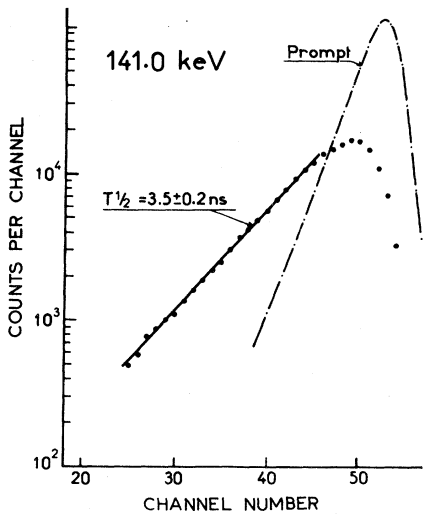

FIG. 5. Time-correlation curve of the 141 keV γ ray measured in the ^{92}Mo + ^{12}C reaction at 50 MeV.

1. *The positive parity band* $(vh_{11/2}\otimes\pi p_{1/2})$

This $\Delta I=2$ decoupled band previously observed in ^{106}Ag (the peaceful case of the two decoupled particles) has not been excited in ^{102,104}Ag. As a matter of fact, the neutron Fermi level moves away from the $vh_{11/2}$ orbital when A is decreasing and such a

TABLE III. Angular distribution and polarization results on γ rays of ^{102}Ag.

E_γ	$I_i \rightarrow I_f$	A_{22}	A_{44}	p	Assigned multipolarity	Mixing ratio δ
40.0	$7^+ \rightarrow 6^+$	−0.33(9)	−0.01(10)		$M1$	$-0.14 \le \delta \le +0.18$
45.9	$7^+ \rightarrow 6^+$	−0.33(9)	−0.02(10)		$M1$	$-0.14 \le \delta \le +0.26$
89.5	$(5^+) \rightarrow (4^+)$	−0.09(3)	−0.10(4)			
97.3	$(4^+) \rightarrow 5^+$	−0.15(7)	−0.08(8)			
141.0	$6^+ \rightarrow 5^+$	+0.54(3)	+0.07(4)	−0.52(9)	$M1/E2$	$-1.7 \le \delta \le -0.7$
148.9	$(6^+) \rightarrow (5^+)$	−0.10(5)	−0.04(6)	−0.17(21)	$M1$	$\delta \sim 0$
157.4	$9^- \rightarrow 8^-$	−0.09(4)	−0.06(5)		$(M1)$	mixed
174.5	$9^+ \rightarrow 8^+$	−0.24(10)	−0.03(13)	−0.04(12)	$M1+E2$	$-0.08 \le \delta \le +0.36$
274.5	$(13,14)^- \rightarrow 13^-$	−0.12(3)	−0.01(4)	−0.28(5)	$M1,E2$	
279.1	$9^+ \rightarrow 8^+$	−0.24(4)	−0.03(4)	−0.29(7)	$M1$	$-0.08 \le \delta \le +0.08$
336.1	$6^+ \rightarrow 5^+$	−0.25(3)	−0.04(3)		$M1\ (+E2)$	
349.5	$11^- \rightarrow 10^-$	−0.18(4)	−0.07(4)	−0.29(6)	$M1$	$-0.08 \le \delta \le +0.05$
397.7	$10^- \rightarrow 9^-$	−0.09(4)	−0.03(3)	−0.32(4)	$M1$	$0 \le \delta \le +0.12$
463.4	$8^+ \rightarrow 7^+$	−0.22(4)	−0.03(5)	−0.33(10)	$M1$	$-0.08 \le \delta \le +0.08$
466.4*	$13^- \rightarrow 12^-$ / $12^- \rightarrow 11^-$	−0.24(3)	−0.02(3)	−0.32(5)	$(M1)$	
539.8	$8^+ \rightarrow 7^+$	−0.10(3)	−0.05(4)	−0.06(4)	$(M1+E2)$	
637.0	$(10^+) \rightarrow 9^+$	−0.23(7)	−0.02(8)		$(M1)$	
664.6	$8^+ \rightarrow 7^+$	+0.55(5)	−0.04(6)	−0.32(12)	$M1+E2$	$-1.7 \le \delta \le +0.08$
705		+0.20(4)	−0.11(6)			
745.7	$10^+ \rightarrow 9^+$	+0.14(10)	+0.02(7)		$(M1+E2)$	
748.0	$11^- \rightarrow 9^-$	+0.27(5)	−0.18(5)		$E2$	
816.5	$12^- \rightarrow 10^-$	+0.10(4)	+0.01(5)	+0.43(4)	$E2$	
819.4	$9^+ \rightarrow 7^+$	+0.19(4)	−0.11(4)		$E2$	
839.1	$9^+ \rightarrow 7^+$	+0.33(3)	−0.10(3)	+0.38(3)	$E2$	
860.9		+0.25(2)	−0.12(3)	+0.36(5)	$(E2)$	
875.9	$11^+ \rightarrow 9^+$	+0.37(3)	−0.11(3)	+0.48(10)	$E2$	
951.0	$13^+ \rightarrow 11^+$	+0.27(3)	−0.12(3)	+0.36(10)	$E2$	
1367.8	$8^- \rightarrow 7^+$	−0.30(3)	−0.02(3)	+0.33(9)	$E1$	$0 \le \delta \le +0.05$

TABLE IV. Angular distribution and polarization results on γ rays of ^{104}Ag.

E_γ	$I_i \rightarrow I_f$	A_{22}	A_{44}	p	Assigned multipolarity	Mixing ratio δ
99.3	$7^+ \rightarrow 6^+$	−0.44(6)	−0.08(5)		$M1+E2$	
112.5	$6^+ \rightarrow 5^+$	−0.12(4)	−0.07(4)		$M1+E2$	
175.3	$9^- \rightarrow 8^-$	−0.27(4)	−0.03(4)	−0.40(6)	$M1$	$-0.03 \le \delta \le +0.02$
316.7	$(8^+) \rightarrow (7^+)$	−0.34(8)	−0.08(7)		$(M1)$	
332.7	$11^- \rightarrow 10^-$	−0.24(5)	−0.02(5)	−0.31(8)	$M1$	$-0.07 \le \delta \le +0.14$
346.2	$10^- \rightarrow 9^-$	−0.29(5)	0.05(6)	−0.55(13)	$M1$	$-0.05 \le \delta \le +0.08$
367.4	$(7^+) \rightarrow 6^+$	−0.24(11)	0.10(10)	−0.47(8)	$M1$	$-0.17 \le \delta \le +0.08$
444.3		−0.31(7)	0.05(6)	−0.32(13)	$M1$	$-0.08 \le \delta \le +0.15$
481.3	$14^- \rightarrow 13^-$	−0.28(9)	−0.01(8)	−0.57(18)	$M1$	$-0.12 \le \delta \le +0.12$
570.1		−0.29(10)	0.01(10)		$(M1)$	
814.6		+0.19(6)	−0.61(13)			
865.1	$8^- \rightarrow 7^+$	−0.41(12)	0.10(10)	0.45(20)	$E1$	$-0.14 \le \delta \le +0.25$
906.8	$(9^+) \rightarrow 7^+$	+0.04(12)	−0.24(11)	0.25(15)	$E2$	
1062.0	$(11^+) \rightarrow (9^+)$	+0.06(11)	0.05(12)	0.6(3)	$(E2)$	

TABLE V. Results on internal conversion coefficients (ICC) measured in ^{102}Ag with the on-line orange spectrometer. Multipolarities and mixing ratios have been deduced.

Transition (keV)	Measured ICC $\times 10^2$	Assigned multipolarity	Mixing ratio $\lvert\delta\rvert$
K 141.0	23.5±6.4	*M*1+*E*2	0.8±0.3
K 148.9	10.0±2.7	*M*2	<0.01
K 157.4	9.0±2.4	*M*1 (+*E*2)	<0.2
L 141.0	4.3±1.1	*M*1+*E*2	0.9±0.4
K 336.4	1.4±0.4	*M*1,*E*2	
K 349.5	1.5±0.4	*M*1,*E*2	
K 397.7	0.8±0.2	*M*1,*E*2	

band is expected at much higher energy in ^{102,104}Ag (around 1.3 MeV).

2. *The negative parity band* ($\nu h_{11/2} \otimes \pi g_{9/2}$)

Three main points have to be discussed:

a. The evolution in the level spacings of the band states depending on the nuclei. In Fig. 8 are shown the negative parity bands observed in ^{102,104,106}Ag with the 10^- states taken at identical energy, in the same way as in Ref. 15. It can be noted that the experimental sequences are quite similar. In Fig. 8 are also reported the results of both rotor plus quasiparticles calculations previously described. It should be noted that our calculation predicts too large energy spacings for high spin sequences which is due to the constant value of the moment of inertia. A better agreement for spins greater than ten is obtained

TABLE VI. Results on ICC measured in ^{104}Ag.

Transition (keV)	Measured ICC $\times 10^2$	Assigned multipolarity	Mixing ratio $\lvert\delta\rvert$
K 99.3	60±10	*M*1+*E*2	0.4±0.2
K 112.5	37± 7	*M*1+*E*2	0.3±0.2
K 175.3	8.4±1.5	*M*1 (+*E*2)	<0.5
K 332.7	1.7±0.5	*M*1,*E*2	
K 346.2	1.0±0.3	*M*1,*E*2	

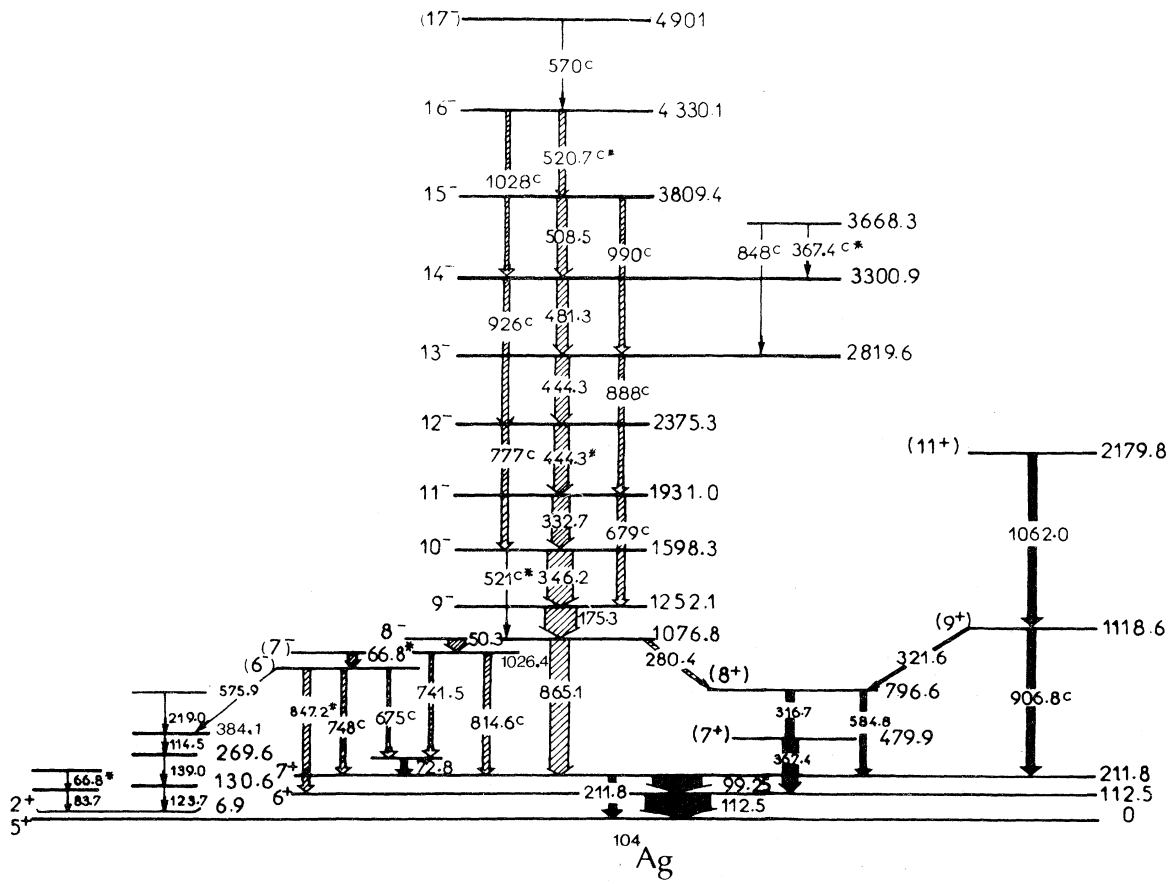

FIG. 6. Decay scheme for the positive and negative parity states in ^{104}Ag excited via the ^{94}Mo + ^{12}C reaction at 50 MeV.

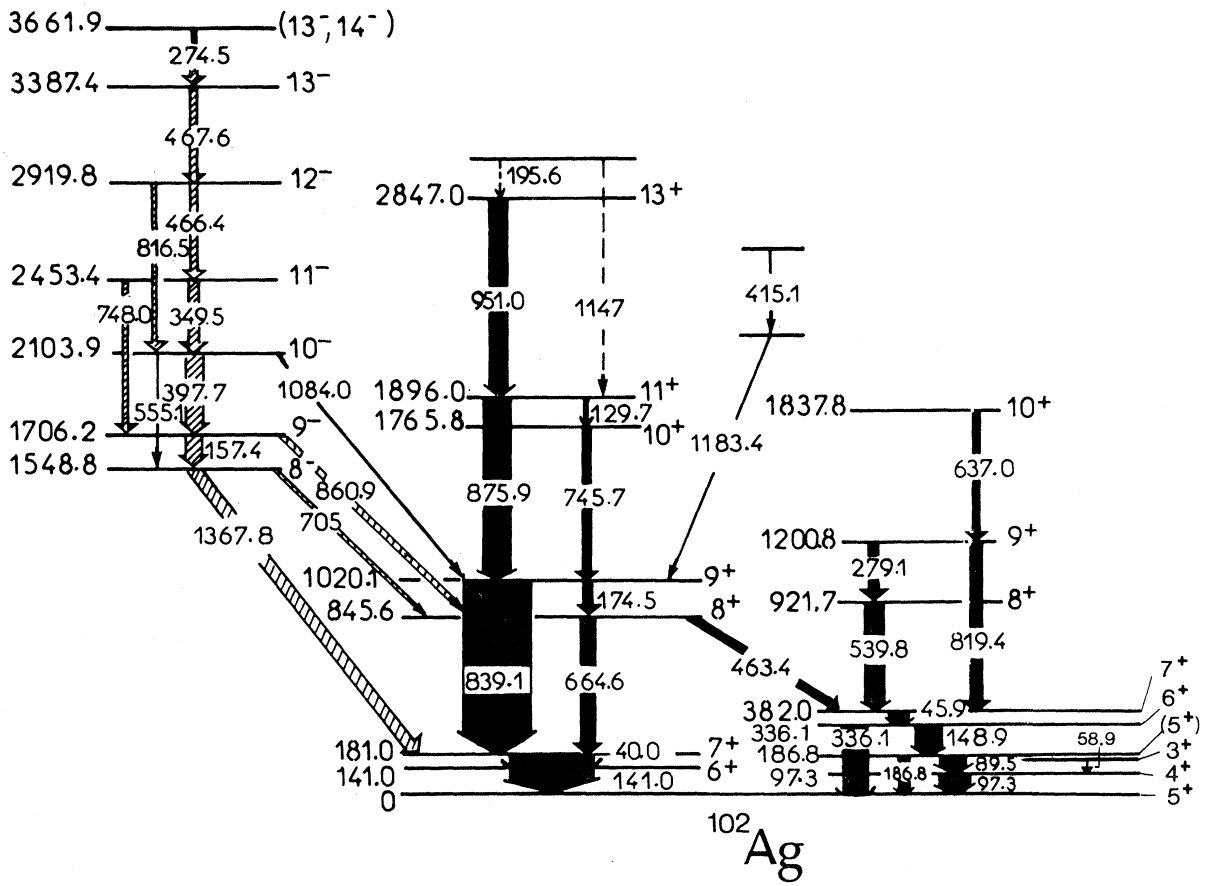

FIG. 7. Level scheme of ^{102}Ag deduced from ^{89}Y + ^{16}O at 60 MeV, ^{92}Mo + ^{14}N at 72 MeV, and ^{92}Mo + 12C at 50 MeV.

through the calculation of Popli *et al.* including a variable moment of inertia. On the other hand, our calculation is much better for spins smaller than ten: The lowest spin levels (as 3^-, 4^-, 5^-) have not been represented by Popli *et al.* because even though they exist, they are not populated by these heavy ion reactions. The 6^-, 7^-, 8^- levels, in both calculations, present a grouping in a 200 keV energy space but are

TABLE VII. K structure of the states of the $\nu h_{11/2}\otimes\pi g_{9/2}$ negative parity band in the standard basis $|IMK\Omega_n\Omega_p\rangle$ of our calculation.

			Weights of the main components of the wave functions									
K value	Ω_n	Ω_p	3^-	4^-	5^-	6^-	7^-	8^-	9^-	10^-	11^-	12^-
2	$\frac{3}{2}h^{11/2}$	$\frac{7}{2}g^{9/2}$	0.31	0.13								
3	$\frac{1}{2}h^{11/2}$	$\frac{7}{2}g^{9/2}$	0.32	0.21	0.09		0.13					
3	$\frac{3}{2}h^{11/2}$	$\frac{9}{2}g^{9/2}$		0.23	0.26	0.22						
4	$\frac{1}{2}h^{11/2}$	$\frac{9}{2}g^{9/2}$		0.16	0.27	0.29	0.21	0.14	0.11	0.09	0.08	0.06
5	$\frac{1}{2}h^{11/2}$	$\frac{9}{2}g^{9/2}$			0.10	0.24	0.27	0.23	0.20	0.18	0.17	0.16
5	$\frac{3}{2}h^{11/2}$	$\frac{7}{2}g^{9/2}$			0.06			0.26	0.26	0.25	0.24	0.23
6	$\frac{3}{2}h^{11/2}$	$\frac{9}{2}g^{9/2}$				0.11	0.23	0.12	0.15	0.16	0.17	0.17
7	$\frac{5}{2}h^{11/2}$	$\frac{9}{2}g^{9/2}$					0.06	0.02	0.04	0.05	0.06	0.06

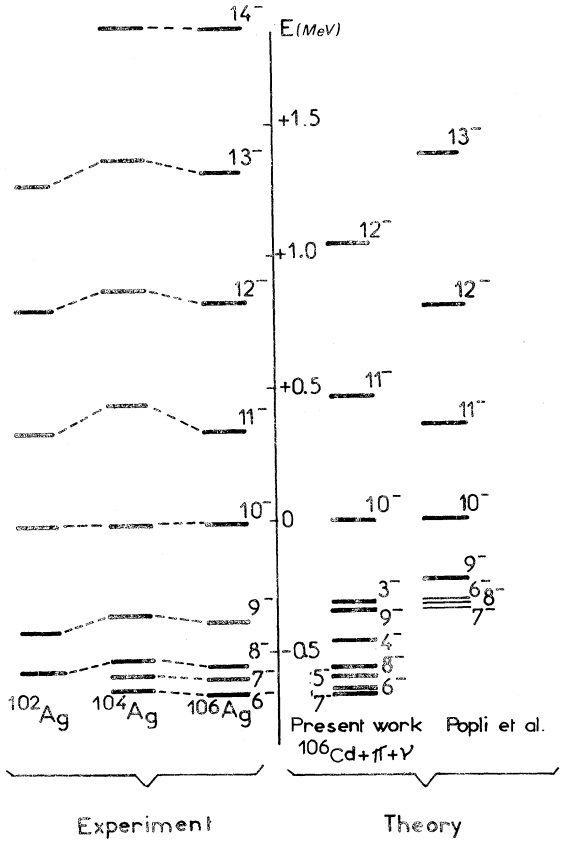

FIG. 8. Comparison of calculated and experimental energies of negative parity states in ^{102,104,106}Ag. Both an experimental and theoretical spectrum for ^{106}Ag has been obtained by Popli *et al.* (Ref. 15).

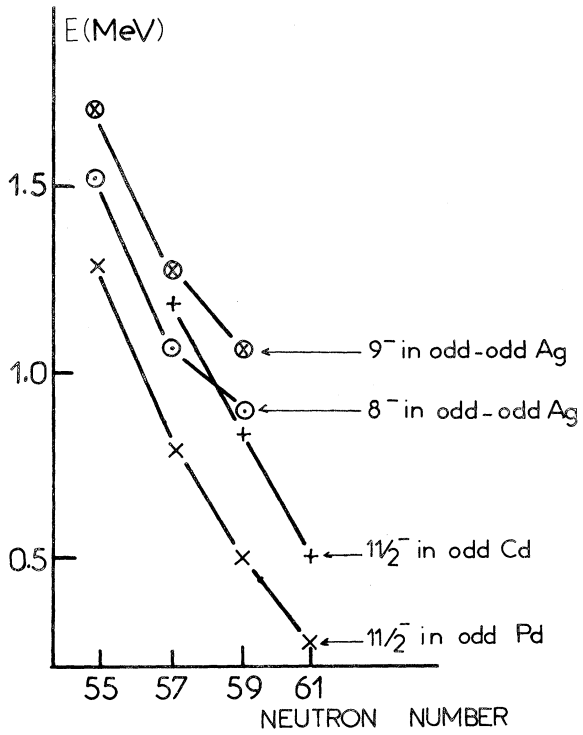

FIG. 9. Variation of experimental energies of the 8^-, 9^-, states in doubly odd Ag and of the $\frac{11}{2}^-$ state in odd neutron Cd and Pd isotopes versus neutron number.

located 300 keV too high in the calculation of Ref. 15; this difference could arise from the choice of the deformed quasiparticle states and from the treatment of the moment of inertia. Thus the results are similar in both works; in particular, the deformation keeps the positive sign (slightly deformed prolate shape). A number of negative states 6^-, 7^-, 8^-,..., are connected to the band and the actual spin of the bandhead is not clear. However, it can be seen in Table VII that the K structures are similar only from the 8^- and following states. The nucleus seems to rotate before the complete alignment $J=j_n+j_p$ is obtained; we will call this conflicting case the real conflicting one.

b. The behavior of the absolute bandhead energy versus A. Assuming that the 8^- state is the bandhead, the variation of its energy versus the neutron number has been compared in Fig. 9 to that of the $\frac{11}{2}^-$ state in neighboring odd-A nuclei. It should be noted that the alteration of the 8^- or 9^- states is quite similar to the behavior of the $\frac{11}{2}^-$ state. Moreover, it has been observed that the negative band is weakly populated in ^{102}Ag in contrast with the strong feeding observed in ^{106}Ag. This situation is consistent with the rising in energy of the $\nu h_{11/2}$ orbital when A is decreasing, which has already been observed in odd Cd (Refs. 11–14) and Pd (Refs. 9 and 10) isotopes.

c. The problem of missing transitions (such as in ^{102}Ag). The question of why the $8^-\rightarrow 7^-\rightarrow 6^-$ transitions are missing in ^{102}Ag while they are observed in ^{104,106}Ag must be approached. A similar phenomenon has been previously noticed in In (Refs. 4 and 5) and Sb.[22] It is possible that these levels are too close in energy (as shown in theoretical calculations) to be populated through gamma decay in ^{102}Ag, the energy spacing of the competing $8^-\rightarrow 7^+$ transition increasing fast from $A=106$ to $A=102$.

As a final remark about this negative parity band, it should be emphasized that the collective rotation corresponds to predominant K values equal to 4,5 (see Tables VII and VI of Ref. 15) or in other words to a mixing of 18% ($J_0=8$), 46% ($J_0=9$), and 33% ($J_0=10$) states as stated in Ref. 15. So we can speak of a real conflicting case because the rotation starts with nonfully aligned particles. However, for very large values of R the decoupling of the proton in a rotation around the R axis must be expected; this situation has not been observed yet, probably due to

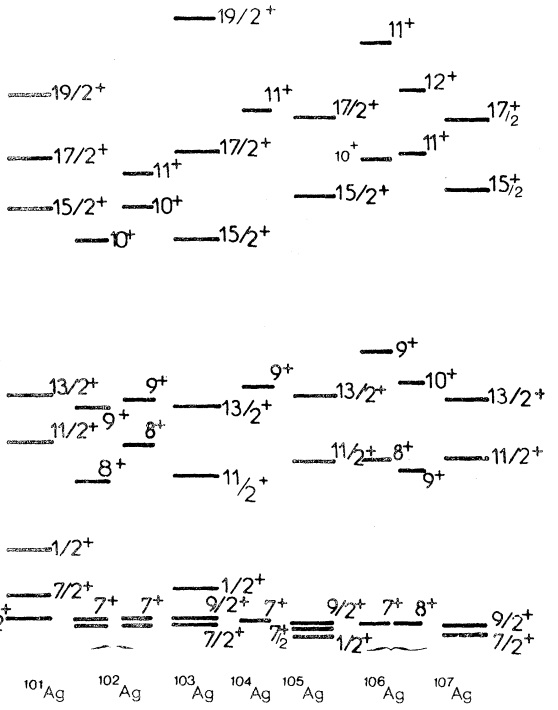

FIG. 10. Comparison of the experimental $\frac{9}{2}^+$ band observed in odd $^{101-107}$Ag with positive parity bands identified in the present work (^{102}Ag and ^{104}Ag and that of Popli *et al.* (Ref. 15) (^{106}Ag).

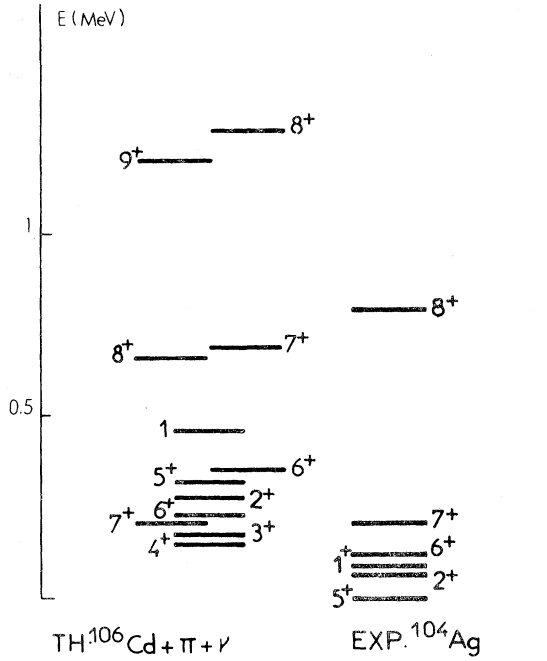

FIG. 11. Comparison of calculated and experimental positive parity states in ^{104}Ag. The zero energy has been adjusted so that the 7^+ levels are at the same excitation energy.

competition of multiparticle excitations arising at such high energy.

3. *The positive parity bands ($\nu g_{7/2}\otimes\pi g_{9/2}$) and ($\nu d_{5/2}\otimes\pi g_{9/2}$)*

A striking analogy between odd and odd-odd Ag level schemes can be seen in Fig. 10 where positive parity levels are separated into two bands built on 7^+ ($\nu d_{5/2}\otimes\pi g_{9/2}$) and 8^+ or 7^+ ($\nu g_{7/2}\otimes\pi g_{9/2}$) states. The energy level staggerings are similar for odd and doubly odd Ag. That means that the neutron acts as a "spectator." This situation is especially obvious in the 7^+ band in ^{102}Ag where energy spacings are very close to those of the $\frac{9}{2}^+$ band in ^{101}Ag.[8] The level scheme of the odd-odd nucleus is then obtained by simple addition of the momentum $j_n=\frac{5}{2}$. In this case, the initial conflicting scheme seems to become a "new peaceful" case with $J=K=j_p+j_n$.

This "one particle spectator" type of coupling or "new peaceful" case is not as clear for $\nu g_{7/2}$ in the 7^+, 8^+, 9^+ band in ^{102}Ag or 8^+, 9^+, 10^+ in ^{106}Ag. This is due to the Coriolis force which is stronger for $g_{7/2}$ than for $d_{5/2}$. In that case the neutron nearly succeeds in coupling with the proton in a conflicting case as discussed previously. In Fig. 11 are shown the results of our simple calculation for the positive parity bands. Because we have not used the core basis $|IMJR_{j_n}j_p\rangle$, the ($\nu g_{7/2}\otimes\pi g_{9/2}$) and ($\nu d_{5/2}\otimes\pi g_{9/2}$) states are not separated. The 5^+, 6^+, 2^+, 7^+ states are found to be very close, as observed in ^{104}Ag, although the 5^+ state lies somewhat too high. However, a good description of the positive parity levels would require the use of the core basis as done by Popli *et al.* for ^{106} Ag.[15] They clearly demonstrated that the $\Delta I=1$ band built on the 7^+ state is due to the fully aligned (84%) ($\nu d_{5/2}\otimes\pi g_{9/2}$) configuration with dominant $\Delta I=2$ transitions, while the $\Delta I=1$ band built on the 8^+ state is given by the ($\nu g_{7/2}\otimes\pi g_{9/2}$) configuration with only 60% of alignment and where $\Delta I=1$ and 2 transitions are both present. By analogy these two bands seem to be present also in $^{102-104}$Ag. However, in ^{102}Ag the ($\nu g_{7/2}\otimes\pi g_{9/2}$) rotational band begins at state 7^+ and not 8^+ because it is an intermediate case between the conflicting case (such as $\nu h_{11/2}\otimes\pi g_{9/2}$) and the new peaceful one (such as $\nu d_{5/2}\otimes\pi g_{9/2}$).

As a concluding remark, these two bands are, however, very mixed; thus it appears necessary to use a realistic residual interaction V_{pn} to mix such positive bands and also to mix ($\nu_{\text{parity}-}\otimes\pi_{\text{parity}-}$) with ($\nu_{\text{parity}+}\otimes\pi_{\text{parity}+}$) states. For example the 5^+ state in ^{106}Ag would be composed of

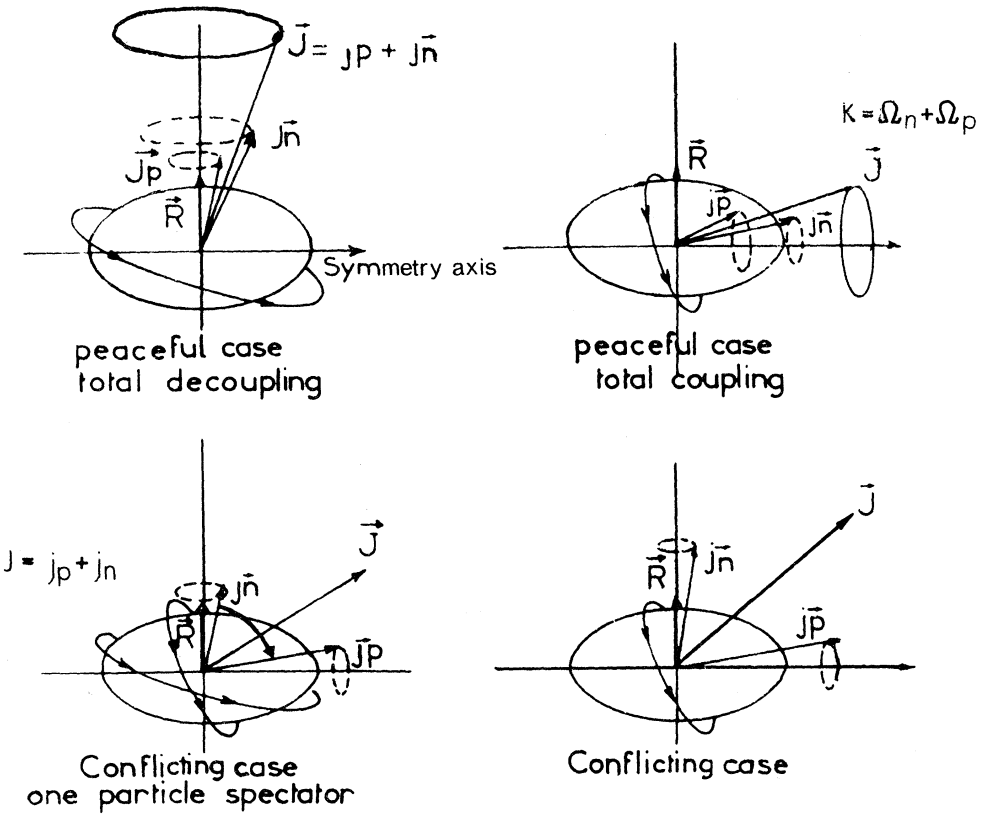

FIG. 12. Extreme cases of coupling scheme occurring in transitional odd-odd nuclei.

$(\nu g_{7/2}\otimes\pi g_{9/2})$, $(\nu d_{5/2}\otimes\pi g_{9/2})$, and $(\nu h_{11/2}\otimes\pi p_{1/2})$ configurations and not only of the $(\nu h_{11/2}\otimes\pi p_{1/2})$ one. Such a simple structure as reported by Popli *et al.* would lead to a strong forbiddenness in the decay of the 5^+ state in ^{106}Ag which has not been observed in experiments.

4. Some general rules of the rotational motion in transitional odd-odd nuclei

In light of these studies concerning the high spin structure of odd-odd Ag and other recent investigations on the same subject (odd-odd In, Tl...,) some general rules can be stated. In Fig. 12 are gathered the different types of coupling occurring in doubly odd nuclei. The so-called peaceful case includes both total coupling (like in the rare-earth region) and total decoupling such as $(\pi h_{11/2}{}^{-1})\otimes(\nu i_{13/2}{}^{-1})$ in Au nuclei[2] or $(\nu h_{11/2}\otimes\pi p_{1/2})$ in ^{106}Ag.[15] In the "conflicting case," two situations are possible. If the decoupled orbital has a high j, with low Ω, the Coriolis force is strong enough to couple the proton and neutron in a real conflicting case such as in indium and silver $(\nu h_{11/2}\otimes\pi g_{9/2})$ and thallium $(\nu i_{13/2}{}^{-1}\otimes\pi h_{9/2})$. The rotation seems to start with the two-particle configurations not being stretched. On the other hand, if the decoupled particle has a lower j, with intermediate Ω (such as $d_{5/2}$ with $\Omega=\frac{3}{2}$) its angular momentum aligns along the symmetry axis of the nucleus but remains as a "spectator." The energy spectrum is then approximately that of the adjacent odd A nuclei and the angular momenta are obtained by simple addition of I odd with the j of the spectator particle (see the typical 7^+ band built on the $\nu d_{5/2}\otimes\pi g_{9/2}$ in ^{102}Ag). Between this new peaceful case deriving from the initial conflicting case and the real conflicting case, intermediate schemes can be observed (such as $\nu g_{7/2}\otimes\pi g_{9/2}$) in silver.

As a conclusion, it must be emphasized that odd-odd Ag can be successfully interpreted as a slightly prolate rotator coupled to one quasineutron and one quasiproton. The two striking results of our study are the confirmation of the negative parity band $(\nu h_{11/2}\otimes\pi g_{9/2})$ in the more deficient silver isotopes, and the existence of a new coupling scheme, deriv-

ing from the conflicting case, observed typically in ^{102}Ag.

However, a realistic interaction V_{pn} is now required to improve the agreement with experiment for the positive parity bands and also to perform a correct mixing of $(-\otimes-)$ and $(+\otimes+)$ configurations as discussed before. In order to eliminate a number of parameters (attenuation of Coriolis matrix elements, β_2,χ,μ, Nilsson states, etc.) a microscopic odd-odd model using the same force for describing the core properties and the proton-neutron interaction is highly desirable. Such calculations using the SIII Skyrme force are in progress.

[1]A. Faessler, in *Future Directions in Studies of Nuclei Far From Stability,* edited by J. H. Hamilton *et al.* (North-Holland, Amsterdam, 1980), pp. 1–14, and references therein.

[2]A. Neskakis, R. M. Lieder, H. Beuscher, Y. Gono, D. R. Haenni, M. Müller-Veggian, and C. Mayer-Böricke, Phys. Lett. 80B, 194 (1979).

[3]A. J. Kreiner, M. A. J. Mariscotti, C. Baktash, E. Der Mateosian, and P. Thieberger, Phys. Rev. C 23, 748 (1981), and references therein.

[4]R. Béraud, A. Charvet, R. Duffait, M. Meyer, J. Genevey, J. Tréherne, F. Beck, and T. Byrski, J. Phys. (Paris) C 10, 159 (1980).

[5]N. Elias, R. Béraud, A. Charvet, R. Duffait, M. Meyer, S. André, J. Genevey, S. Tedesco, J. Tréherne, F. Beck, and T. Byrski, Nucl. Phys. A351, 142 (1981).

[6]R. Popli, J. A. Grau, S. I. Popik, L. E. Samuelson, F. A. Rickey, and P. C. Simms, Phys. Rev. C 20, 1350 (1979).

[7]J. Tréherne, J. Genevey, R. Béraud, A. Charvet, R. Duffait, M. Meyer, F. A. Beck, and T. Byrski, Nucl. Phys. A342, 357, (1980).

[8]A. W. B. Kalshoven, J. J. Van Ruyven, W. H. A. Hesselink, J. Ludziejewski, H. Verheul, and M. J. A. De Voigt, Nucl. Phys. A346, 147 (1980).

[9]H. A. Smith, Jr. and F. A. Rickey, Phys. Rev. C 14, 1946 (1976).

[10]J. S. Kim, Y. K. Lee, K. A. Hardy, P. C. Simms, J. A. Grau, G. J. Smith, and F. A. Rickey, Phys. Rev. C 12, 499 (1975).

[11]M. Meyer, R. Béraud, A. Charvet, R. Duffait, J. Tréherne, and J. Genevey, Phys. Rev. C 22, 589 (1980).

[12]J. Genevey, J. Tréherne, J. Danière, R. Béraud, M. Meyer, and R. Rougny, J. Phys. G 4, 943 (1978).

[13]M. Meyer, R. Béraud, J. Daniére, R. Rougny, J. Genevey, J. Tréherne, and D. Barnéoud, Phys. Rev. C 12, 1858 (1975).

[14]D. C. Stromswold, D. O. Elliot, Y. K. Lee, L. E. Samuelson, J. A. Grau, F. A. Rickey, and P. C. Simms, Phys. Rev. C 17, 143 (1978).

[15]R. Popli, F. A. Rickey, L. E. Samuelson, and P. C. Simms, Phys. Rev. C 23, 1085 (1981).

[16]Institut de Physique Nucléaire de Lyon, Rapport Annuel, 1981 LYCEN-Report-8201 and 1982 LYCEN-Report-8231.

[17]S. André, J. Tréherne, and D. Barnéoud, J. Phys. (Paris) Lett. 18, 369, (1977); and S. Tédesco, thesis, Grenoble, 1979.

[18]L. C. Biedenharn and M. E. Rose, Rev. Mod. Phys. 25, 729 (1953).

[19]J. Ludziejewski, J. Bron, W. H. A. Hesselink, A. W. B. Kalshoven, L. K. Peker, A. Van Poelgeest, and H. Verheul, Nucl. Phys. A344, 283 (1980).

[20]M. Meyer, J. Danière, J. Letessier, and P. Quentin, Nucl. Phys. A316, 93 (1979).

[21]J. Libert, M. Meyer, and P. Quentin, Phys. Lett. 95B, 175 (1980).

[22]R. Duffait, J. Van Maldeghem, A. Charvet, J. Sau, K. Heyde, A. Emsallem, M. Meyer, R. Béraud, J. Tréherne, and J. Genevey, Z. Phys. 307, 259 (1982).